Alternate Substrate Binding Modes to Two Mutant (D98N and H255N) Forms of Nitrite Reductase from *Alcaligenes faecalis* S-6: Structural Model of a Transient Catalytic Intermediate[†,‡]

Martin J. Boulanger[§] and Michael E. P. Murphy*[,§,||]

Departments of Biochemistry & Molecular Biology and of Microbiology & Immunology, The University of British Columbia, Vancouver, BC V6T 1Z3, Canada

Received April 11, 2001; Revised Manuscript Received May 31, 2001

ABSTRACT: High-resolution nitrite soaked oxidized and reduced crystal structures of two active site mutants, D98N and H255N, of nitrite reductase (NIR) from *Alcaligenes faecalis* S-6 were determined to better than 2.0 Å resolution. In the oxidized D98N nitrite-soaked structures, nitrite is coordinated to the type II copper via its oxygen atoms in an asymmetric bidentate manner; however, elevated *B*-factors and weak electron density indicate that both nitrite and Asn98 are less ordered than in the native enzyme. This disorder likely results from the inability of the Nδ2 atom of Asn98 to form a hydrogen bond with the bound protonated nitrite, indicating that the hydrogen bond between Asp98 and nitrite in the native NIR structure is essential in anchoring nitrite in the active site for catalysis. In the oxidized nitrite soaked H255N crystal structure, nitrite does not displace the ligand water and is instead coordinated in an alternative mode via a single oxygen to the type II copper. His255 is clearly essential in defining the nitrite binding site despite the lack of direct interaction with the substrate in the native enzyme. The resulting pentacoordinate copper site in the H255N structure also serves as a model for a proposed transient intermediate in the catalytic mechanism consisting of a hydroxyl and nitric oxide molecule coordinated to the copper. The formation of an unusual dinuclear type I copper site in the reduced nitrite soaked D98N and H255N crystal structures may represent an evolutionary link between the mononuclear type I copper centers and dinuclear Cu_A sites.

In dissimilatory denitrification, nitrate and nitrite are used as electron acceptors in anoxic respiration and are reduced to gaseous nitrogen oxide compounds (NO, N_2O) and dinitrogen (N_2) (*2, 3*). Nitrite reductases (NIRs)[1] are common to many facultative anaerobic bacteria and catalyze the first committed step in this pathway. Copper-containing NIRs (CuNIRs) have been identified primarily in Gram-negative (*4*−*7*) bacteria but also occur in Gram-positive bacteria (*8*) and fungi (*9*), catalyzing the one-electron reduction of nitrite to nitric oxide under anaerobic conditions. Two distinct classes of NIRs exist that contain either heme *c* and heme d_1 prosthetic groups or multiple copper centers (CuNIR) [reviewed in (*3*)]. The dissimilatory pathway is responsible for generating the only biological source of dinitrogen (N_2) (*3*).

NIR from *Alcaligenes faecalis* strain S-6 (AfNIR) is a green 110 kDa soluble periplasmic homotrimer with each monomer comprising two Greek key β-barrel domains of the cupredoxin fold family (*10, 11*). Each monomer contains one type I copper coordinated by four protein ligands (His95, Cys136, His145, and Met150) in a distorted trigonal bipyramidal geometry and one type II copper that adopts a tetrahedral coordination with three histidine ligands (His100, His135, and His306) and a fourth solvent ligand. Each copper type exhibits unique spectroscopic signatures. The type I copper in AfNIR shows visible absorbance at 458 and 585 nm resulting in a green-colored protein (*5, 11*). The two copper sites are approximately 12.5 Å apart and are intimately linked through a Cys−His bridge incorporating the type I ligand Cys136 and the type II ligand His135. This linkage of the copper centers provides an efficient electron-transfer pathway during catalysis, consistent with a first-order electron-transfer rate of 1.4×10^3 s^{-1} measured by pulse radiolysis on NIR from *Achromobacter cycloclastes* (AcNIR) (*12*). Crystallography (*10, 13, 14*) and electron nuclear double resonance (ENDOR) spectroscopy (*15, 16*) have shown that nitrite displaces the ligand water at the type II site in oxidized CuNIR. In the reduced state, the ligand water is lost, and

[†] This work is supported by a research grant from the National Science and Engineering Research Council of Canada (to M.E.P.M.). M.J.B. is supported by a University Graduate Fellowship. M.E.P.M. is a Medical Research Council of Canada Scholar.

[‡] The atomic coordinates for oxidized D98N[NO_2^-], reduced D98N[NO_2^-], oxidized H255N[NO_2^-], and reduced H255N[NO_2^-] AfNIR have been deposited in the Protein Data Bank (file codes: 1J9Q, 1J9R, 1J9S, and 1J9T, respectively).

* To whom correspondence should be addressed. Telephone: 604-822-8022. FAX: 604-822-6041. E-mail: memurphy@interchange.ubc.ca.

[§] Department of Biochemistry & Molecular Biology.

[||] Department of Microbiology & Immunology.

[1] Abbreviations: NIR, nitrite reductase; CuNIR, copper-containing nitrite reductase; AfNIR, *Alcaligenes faecalis* S-6 NIR; D98N[NO_2^-], nitrite soaked D98N AfNIR mutant; H255N[NO_2^-], nitrite soaked H255N AfNIR mutant; AxNIR, *Alcaligenes xylosoxidans* NIR; AcNIR, *Achromobacter cycloclastes* NIR; RsNIR, *Rhodobacter sphaeroides* NIR; FT-IR, Fourier transform infrared spectroscopy; EPR, electron paramagnetic resonance; EXAFS, X-ray fine absorption spectroscopy.

10.1021/bi0107400 CCC: $20.00
Published on Web 07/14/2001

the enzyme displays weaker nitrite binding as shown by crystallography (*14*), X-ray absorption fine spectroscopy (EXAFS), and steady-state kinetics (*17*). Direct binding of nitrite to the type II copper in the active site of *Alcaligenes xylosoxidans* NIR (AxNIR) results in a lengthening of the copper−histidine ligand distances (Δ0.08 Å) (*18*) acting as a possible trigger for electron transfer from the type I copper (*17*). Cyclic voltammetry and EPR spectroscopy (*19*) on NIR from *Rhodobacter sphaeroides* (RsNIR) suggest that intramolecular electron transfer is less favorable in the absence of nitrite. Together these data are consistent with a proposed catalytic mechanism (*13, 14*) that proceeds by an ordered process where nitrite binds to the oxidized type II copper center followed by electron transfer from the type I center.

Analysis of the crystal structure of AcNIR suggested that two residues, Asp98 and His255, which are observed to be close but not ligating to the type II copper are likely involved in catalysis by shuttling protons to the reaction center (*10, 13*). In the native nitrite soaked AfNIR structure, the side chain of Asp98 forms a well-defined hydrogen bond to an oxygen atom of the nitrite that is asymmetrically O-coordinated to the type II copper (*14*). Asp98 is also closely linked with His255 through a highly conserved water-bridged hydrogen bond. Additional evidence for the importance of these residues is derived from modeling studies with AxNIR that indicate Asp98 and His255 are structurally analogous to catalytically important residues in Zn−Cu SOD (*18*). Recently, the catalytic significance of both Asp98 and His255 has been demonstrated by site-directed mutagenesis (*19*−*21*). Mutations of these residues in three different CuNIRs showed greater than 100-fold reduction in specific activity (*16, 20*) and significantly reduced affinity for nitrite (*16, 19, 21*).

To understand better the roles of the active site residues Asp98 and His255 in nitrite binding and catalysis in AfNIR, we report the nitrite soaked crystal structures of two active site mutants, D98N[2] and H255N, in both the oxidized and reduced forms. Both Asp98 and His255 are found to be essential in determining the binding mode of nitrite in the active site of AfNIR. The oxidized D98N[NO_2^-] crystal structure indicates that Asp98 in the native enzyme serves as a proton acceptor in forming a hydrogen bond with nitrite and is essential for productive substrate binding. A restructured solvent network results in a unique pentacoordinate binding mode of nitrite in the oxidized H255N[NO_2^-] structure that provides a structural model for a proposed transient catalytic intermediate. In the reduced D98N[NO_2^-] and H255N[NO_2^-] structures, a unique dinuclear site is formed in the type I copper site and shows structural similarities to the traditional Cu_A site.

EXPERIMENTAL PROCEDURES

Molecular Biology. The D98N and H255N mutations were constructed by site-directed mutagenesis and cloned in pUC19 (New England Biolabs) as described previously (*11*). Expression in *Escherichia coli* followed by cell lysis and protein purification by a nickel affinity column and FPLC ion exchange chromatography results in a protein preparation greater than 95% pure. This procedure produces AfNIR protein with the correct molecular mass, full copper occupation, and similar specific activity to native AfNIR (*20*).

Crystallization, Soaking, and Data Collection. D98N and H255N crystals were grown at room temperature by the hanging drop vapor diffusion method with equal volumes (3 μL) of mother liquor and protein solution. The mother liquor consisted of 0.1 M sodium cacodylate, pH 5.5, 0.1 M sodium acetetate, pH 4.7, 10−15% poly(ethylene glycol) (PEG) 6000, and equimolar concentrations of cupric chloride (5 mM) and zinc acetate (5 mM). The protein stock used in crystallization was 10 mg/mL buffered in 10 mM Tris, pH 7.0. These conditions resulted in green crystals that grew to dimensions of 0.3 mm × 0.5 mm × 0.5 mm within 1 week. High concentrations of zinc ion (50 mM) in the crystallization mix produced AfNIR crystals in space group *R3* (*20*); however, lower zinc ion concentrations (≤5 mM) combined with equimolar amounts of copper ion result in orthorhombic crystals of space group $P2_12_12_1$ that are isomorphous with previous AfNIR crystals (*11, 14, 22*).

Nitrite soaked oxidized crystals were obtained by placing crystals in mother liquor supplemented with 5 mM sodium nitrite for 45 min at room temperature. The crystals were then transferred to fresh mother liquor supplemented with 5 mM nitrite and 30% glycerol as a cryo-protectant. Initial attempts at reducing nitrite soaked crystals with ascorbate at room temperature resulted in the crystals reoxidizing and turning green within 20 min. Reduced, colorless nitrite soaked crystals were ultimately obtained by soaking crystals in mother liquor supplemented with 5 mM nitrite at 0 °C for 45 min followed by an increasing stepwise gradient of freshly prepared ascorbate from 1 mM to 5 mM to 20 mM over 1 h. The AfNIR mutants are 100−1000-fold less active than the wild-type enzyme, and soaking crystals at 0 °C minimized turnover of the enzyme such that no observable reoxidation of the type I copper occurred during this period. Reduced nitrite soaked crystals were fragile and required a 10% stepwise addition of glycerol to a final concentration of 30% over 5 min. Crystals were looped directly into a cryostream at 100 K generated by a cryostat (Oxford Cryo Systems, Oxford, U.K.). X-ray data were collected on a Rigaku R-AXIS IIc image plate system with Cu Kα radiation generated by a Rigaku RU 300 rotating anode operating at 100 mA and 50 kV and focused with Osmic confocal max-flux optical mirrors. All data sets were collected to at least 2.0 Å resolution and processed with DENZO (*23*). Data collection statistics are summarized in Table 1.

Structure Solution and Refinement. The D98N and H255N crystals used for the soaking experiments grew in a primitive orthorhombic lattice and contain the assembled trimer in the asymmetric unit. The nitrite soaked native AfNIR structure (*14*) was used as the starting model for both the oxidized D98N[NO_2^-] and H255N[NO_2^-] crystal structures following removal of the mutated residues, all solvent atoms, and the nitrite. These oxidized mutant structures were used as the starting models for their respective reduced nitrite soaked structures. The final structure of each mutant begins at Ala4 and ends at Glu339. Ten percent of the data was set aside for calculation of the free *R*-factor (*24*). Standard CNS (*25*) maximum likelihood positional and *B*-refinement was carried out with solvent being added with the WATERPICK procedure, resulting in an R_{work} below 19% and an R_{free} of

[2] The amino acid numbering is that of AcNIR based on the sequence alignment by Nishiyama et al. (*1*).

Table 1: Data Collection and Refinement Statistics

crystal	oxidized D98N[NO_2^-]	reduced D98N[NO_2^-]	oxidized H255N[NO_2^-]	reduced H255N[NO_2^-]
cell dimensions (Å)	$a = 61.92$	$a = 61.43$	$a = 62.00$	$a = 61.63$
	$b = 102.5$	$b = 102.3$	$b = 102.4$	$b = 102.2$
	$c = 145.8$	$c = 145.9$	$c = 146.3$	$c = 146.0$
resolution (Å)	1.65 (1.75−1.65)[a]	2.00 (2.13−2.00)	1.90 (2.02−1.90)	1.95 (2.07−1.95)
R-merge	0.064 (0.251)	0.062 (0.294)	0.066 (0.143)	0.071 (0.292)
$\{I\}/\{\sigma(I)\}$[b]	13.4 (2.63)	19.6 (4.25)	19.8 (5.35)	14.6 (3.96)
completeness (%)	88.6 (83.3)	97.6 (95.5)	90.0 (70.1)	96.5 (98.2)
unique reflections	84714 (14072)	61451 (9867)	66707 (8527)	67729 (11357)
redundancy	5.31	9.68	7.71	7.74
working *R*-factor	0.178	0.186	0.164	0.179
free *R*-factor	0.210	0.225	0.203	0.218
rmsd bond length (Å)	0.010	0.006	0.008	0.008
overall *B*-factor ($Å^2$)[c]	17.6	26.2	17.8	21.8
PDB entry code	1J9Q	1J9R	1J9S	1J9T

[a] Values in parentheses are for the highest resolution shell. [b] $\{I\}/\{\sigma(I)\}$ is the average intensity divided by the average estimated error in intensity. [c] *B*-factors are an average from all three monomers.

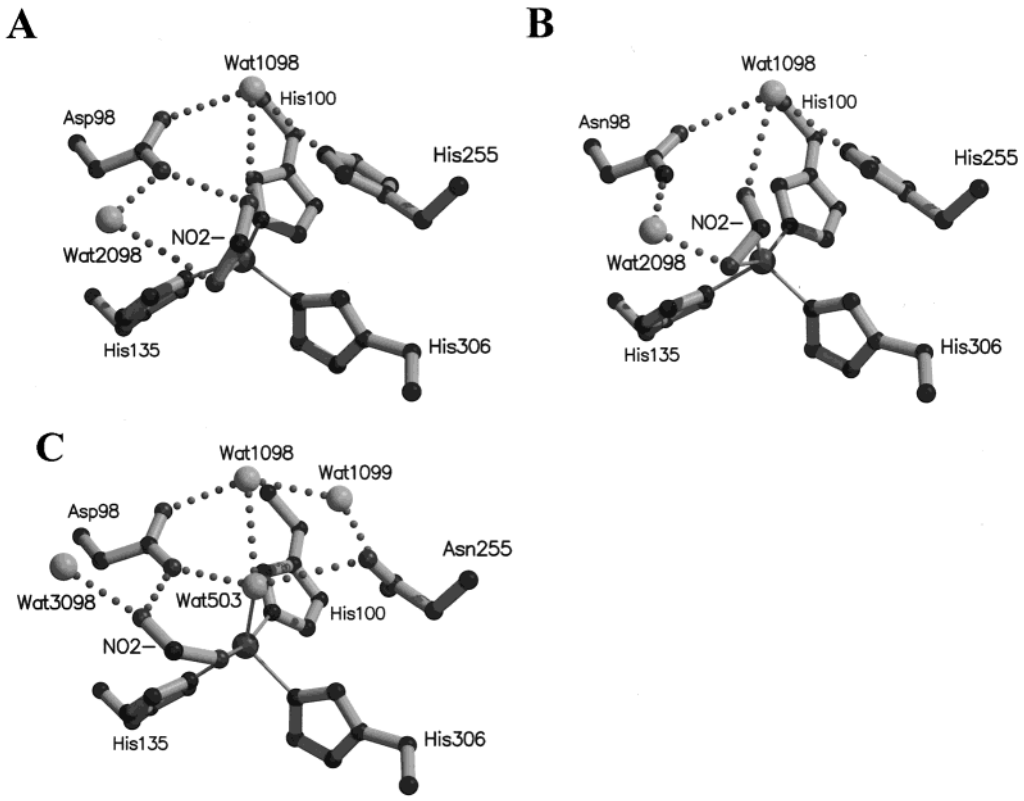

FIGURE 1: Stick diagram showing the orientation of nitrite in the active site of (A) nitrite soaked native AfNIR (*14*), (B) oxidized D98N[NO_2^-], and (C) oxidized H255N[NO_2^-] structures. The type II copper is coordinated by histidines 100, 135, and 306. Hydrogen bonds are depicted as dotted lines. Molscript (*35*) and Raster 3D (*36*) were used to prepare Figures 1−3.

less than 22% in each of the four structures. During refinement, the interactions between copper and nitrite and between copper and the polypeptide were not restrained. Over 90% of the residues in each structure occupy the most favorable position with the remaining residues in the allowed regions in the Ramachandran plot as described by PROCHECK (*26*). Manual intervention was accomplished using the visualization program O (*27*). Final refinement statistics are presented in Table 1.

RESULTS

Native Active Site. The active site of AfNIR is located at the bottom of a 16 Å deep cavity at the interface of two adjacent subunits. The type II copper is coordinated by two histidines (His100, His135) from one subunit, a third histidine (His306) from the adjacent subunit, and a solvent ligand. In the native enzyme, Asp98 is oriented to form a hydrogen bond with the ligand water and interacts with His255 through a single water-bridged hydrogen bond (*11*, *22*). This bridging water completes a solvent network extending to His260 that sits on the surface of AfNIR (*22*). In the nitrite soaked AfNIR crystal structure (*14*), nitrite displaces the ligand water, interacts with the type II copper in an asymmetric manner through the oxygen atoms, and hydrogen-bonds with Asp98 (Figure 1A). No hydrogen bond between nitrite and His255 is observed in the native nitrite soaked structure. Two hydrophobic residues (Ile257 and Leu308) are within 5 Å of the bound nitrite and may serve as important determinants

Table 2: Active Site Ligand and Hydrogen Bond Distances

parameter	oxidized D98N[NO_2^-]	reduced D98N[NO_2^-]	oxidized H255N[NO_2^-]	reduced H255N[NO_2^-]
	I. Type II Cu−Ligand Distances (Å)			
Cu502−100Nϵ2	2.00 (0.01)[a]	2.00 (0.04)	2.04 (0.06)	2.01 (0.02)
Cu502−135Nϵ2	2.08 (0.04)	2.14 (0.01)	2.19 (0.02)	2.10 (0.03)
Cu502−306Nϵ2	2.06 (0.03)	2.16 (0.02)	2.19 (0.01)	2.16 (0.02)
Cu502−503OH_2	N/A	N/A	2.15 (0.09)	1.70 (0.25)
	II. Type II Cu−Nitrite Distances (Å)			
Cu502−N	2.32 (0.18)	2.27 (0.014)	3.21 (0.13)	3.70 (0.05)
Cu502−O1	2.42 (0.05)	2.89 (0.48)	3.60 (0.15)	4.02 (0.16)
Cu502−O2	2.21 (0.08)	2.21 (0.19)	2.16 (0.05)	2.57 (0.07)
	III. Active Site Ligand−H-Bond Distances (Å)			
504O2−1098OH_2	3.50 (0.27)	3.47 (0.24)	N/A	N/A
Asp98$^{O\delta2}$−504O1	N/A	N/A	2.79 (0.19)	2.81 (0.08)
Asp98$^{O\delta2}$−503OH_2	N/A	N/A	2.91 (0.24)	2.36 (0.01)
503OH_2−1098OH_2	N/A	N/A	3.45 (0.06)	4.27[b] (0.22)

[a] Bond distances are an average of all three monomers. [b] Greater than accepted hydrogen bonding distance.

in substrate binding (*13*, *22*). Residues Ala137, Val142, Val146, and Phe312 complete the active site hydrophobic pocket that extends out along one side of the cavity to the molecular surface.

Mutant Active Sites. In the oxidized D98N[NO_2^-] structure, nitrite is also coordinated to the type II copper in a bidentate manner via the oxygen atoms (Figure 1B). Although the coordination is similar to that observed in the native structure, the position of the nitrite N atom relative to the copper is altered. In the mutant, the nitrite nitrogen is positioned almost perpendicular to the plane defined by the oxygen atoms and the type II copper, resulting in a severely bent conformation (Figure 1B). In the native nitrite soaked AfNIR structure, a smaller nitrite bend is observed of approximately 30° from the vertical plane defined by the type II copper and the oxygen atoms of the nitrite (*14*), differing from the D98N[NO_2^-] structure by approximately 60°.

A rotation of approximately 20° about the χ_2 torsional angle of Asn98 in the oxidized D98N[NO_2^-] structure results in the Nδ2 atom being displaced by about 0.6 Å relative to the Oδ1 atom of Asp98 in the native structure. Although 2.6 Å away, the reoriented side chain of Asn98 displays poor hydrogen bond geometry with the bound nitrite. The O1 and O2 atoms of the bound nitrite form hydrogen bonds with Wat2098 (2.45 Å) and the bridging water, Wat1098 (3.50 Å), respectively (Figure 1B, Table 2). Asn98 Oδ1 is positioned to form a 3.38 Å hydrogen bond with the bridging water through which it is linked with His255 Nϵ2 (Figure 1B). The Nϵ2 atom of His255 sits 3.32 Å from the closest nitrite atom (O2), but poor geometry limits the formation of a hydrogen bond.

An average *B*-factor of 36.4 Å^2 and omit difference electron density maps indicate that nitrite is poorly ordered in the oxidized D98N[NO_2^-] structure[Figure 2 , D98N(ox)]. Furthermore, the side chain of Asn98 is also disordered, occupying two distinct conformations. The occupancy of each conformer varies between the three different active sites in the crystal asymmetric unit, but in each case the predominant position is directed toward the type II copper. The nitrite may also bind in multiple conformations in the oxidized D98N[NO_2^-] structure; however, only one orientation could be modeled reliably into the somewhat diffuse density.

The altered binding orientation of nitrite in the oxidized D98N[NO_2^-] structure results in a small shift of Ile257 toward the nitrite such that the closest atom, Ile257 Cδ1, is positioned 2.96 Å from the nitrite nitrogen. The shift of Ile257 results in a slightly more occluded substrate binding site. With the exception of the Cδ1 and Cδ2 atoms of Leu308 that are 4.76 and 4.01 Å from the closest atom of nitrite (O1), respectively, all other active site hydrophobic residues are greater than 5.00 Å away [Figure 2, D98N(ox)].

The most surprising feature of the oxidized H255N[NO_2^-] crystal structure is that nitrite binding to the type II copper does not displace the ligand water (Wat503). Instead, nitrite forms a monodentate coordination to the copper through a single oxygen atom, O2 (Figure 1C). In this new binding mode, the nitrite is not bent, but the N atom is positioned parallel with the plane defined by the oxygen atoms and type II copper. Relative to the nitrite soaked native AfNIR structure, the nitrite is displaced away from Ile257 and toward Ala137 by approximately 1.5 Å [Figure 2, H255N(ox)]. The nitrite O1 atom contacts Ile257 Cδ1 (3.49 Å), and the O2 atom is positioned near Ala137 Cβ (3.42 Å). As a result of nitrite binding, the ligand water (Wat503) is shifted approximately 1 Å toward the bridging water (Wat1098). The pentacoordinate type II copper adopts a distorted square pyramidal geometry with His306 at the sole axial position.

The hydrogen bond network surrounding nitrite bound to the active site is altered drastically. The shift of the ligand water allows the formation of hydrogen bonds to the bridging water (3.47 Å) and to the Oδ1 atom of Asn255 (3.49 Å) (Figure 1C). The ligand water maintains a 2.67 Å hydrogen bond with the Oδ2 of Asp98 (Figure 1C). The oxygen atom of nitrite not coordinated to the copper (O1) overlaps approximately with the location of Wat2098 in the nitrite soaked native structure and is anchored through a hydrogen bond (2.61 Å) to Asp98 Oδ2 (Figure 1C). Two new solvent atoms are introduced into the active site, Wat3098 and Wat1099. Wat3098 (*B*-factor 25.9 Å^2) is located near the position of the displaced Wat2098 and is close enough to the nitrite O1 atom (2.70 Å) to form a hydrogen bond. Wat1099 (*B*-factor 18.5 Å^2) results from replacing His255 with the smaller asparagine residue. This extra water hydrogen-bonds with Asn255 and Wat1098, effectively maintaining the solvent network bridge between Asp98 and residue 255 (Figure 1C).

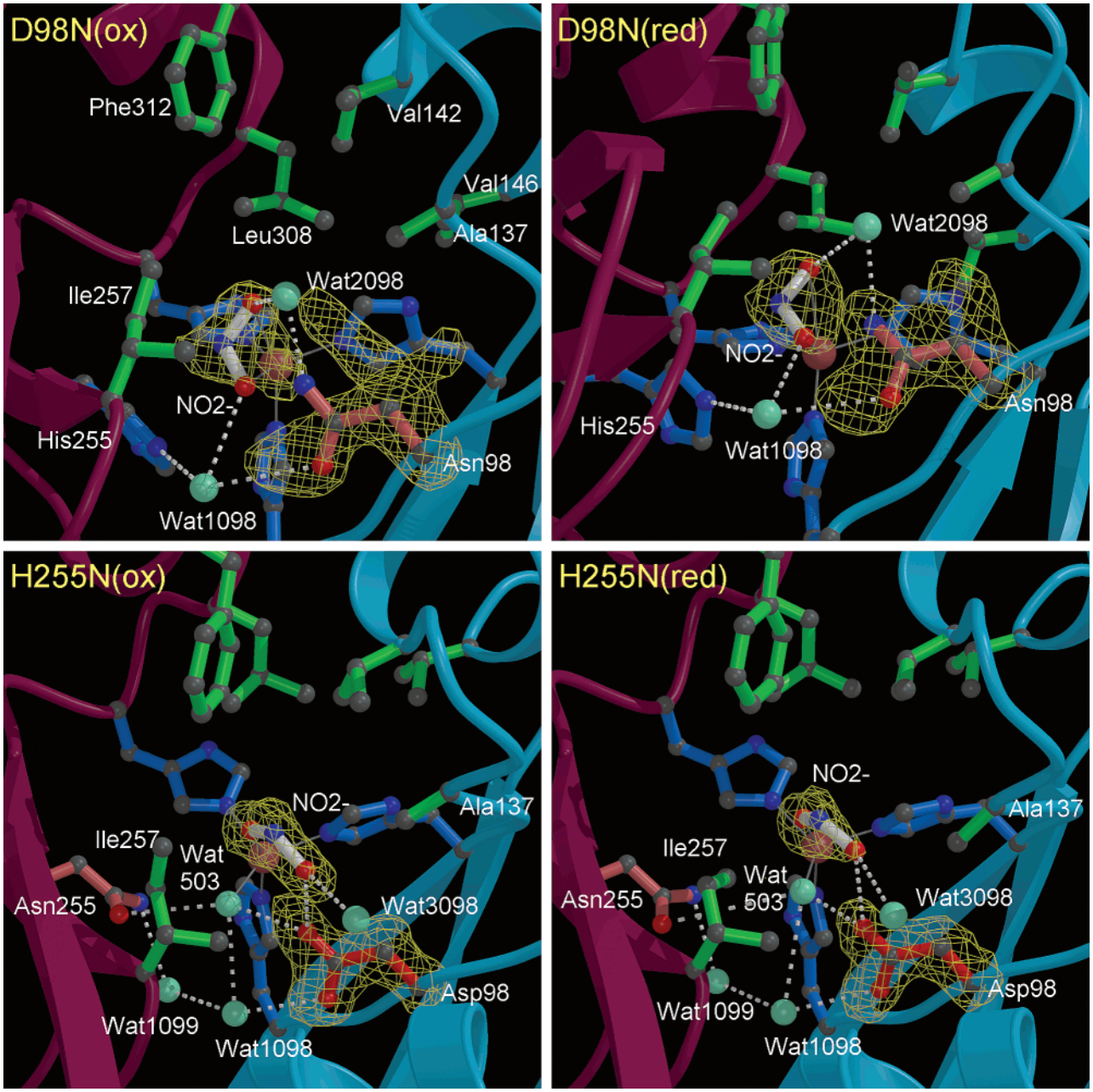

FIGURE 2: Active sites of oxidized D98N[NO_2^-], reduced D98N[NO_2^-], oxidized H255N[NO_2^-], and reduced H255N[NO_2^-] AfNIR mutants. The three histidine type II copper ligands are drawn in blue as is His255 in the top panels. Asn98 (top panels) is colored in light red, as is Asn255 in the bottom panels. Asp98 (bottom panels) is colored in red. Water molecules are drawn as aquamarine spheres. The aliphatic residues Ile257 and Leu308, Val304, Val146, and Val142 are shown in green. Copper atoms are colored gray; nitrogens are colored dark blue and oxygen atoms red. The backbones of monomers C and B are shown in burgundy and teal, respectively. Nitrite bound in the active site is colored. Omit $F_o - F_c$ electron density maps of the nitrite are contoured at 4σ and drawn as a yellow wire mesh. Note the presence of density for two distinct conformations of Asn98 in the oxidized and reduced D98N[NO_2^-] structures.

Data for reduced D98N[NO_2^-] and H255N[NO_2^-] crystals were collected to attempt to identify structures of catalytic intermediates. In these structures, increased *B*-factors and weaker electron density from omit maps [Figure 2, D98N(red), H255N(red)] suggest that nitrite is bound at lower occupancy or is more disordered. The average *B*-factors for nitrite are increased from 32.4 to 37.3 Å^2 and from 23.3 to 45.8 Å^2 upon reduction of the D98N[NO_2^-] and H255N[NO_2^-] structures, respectively. In each structure, however, nitrite adopts a similar position in the active site relative to the oxidized structure (Figure 2). Comparing the reduced and oxidized D98N[NO_2^-] structures, the *B*-factor of the bridging water (Wat1098) that connects Asn98 with His255 shows the greatest increase (35.8 vs 16.9 Å^2). In the reduced H255N[NO_2^-] structure, the side chain of Ile257 adopts a different conformation in the reduced state with the Cδ1 atom directed down toward the type II copper positioned 2.95 Å from the O2 atom of the nitrite [Figure 2, H255N(red)]. Wat3098, which is involved in a hydrogen bond with nitrite in the H255N[NO_2^-] structures, shows a near 2-fold increase (46.2 vs 26.7 Å^2) in *B*-factor in the reduced H255N[NO_2^-] structure as does the ligand water, Wat503 (47.1 vs 28.3 Å^2), indicating increased disorder or reduced occupancy. The ligand water, Wat503, is no longer within hydrogen bonding distance to the bridging water, Wat1098, in the reduced H255N[NO_2^-] structure (Table 2).

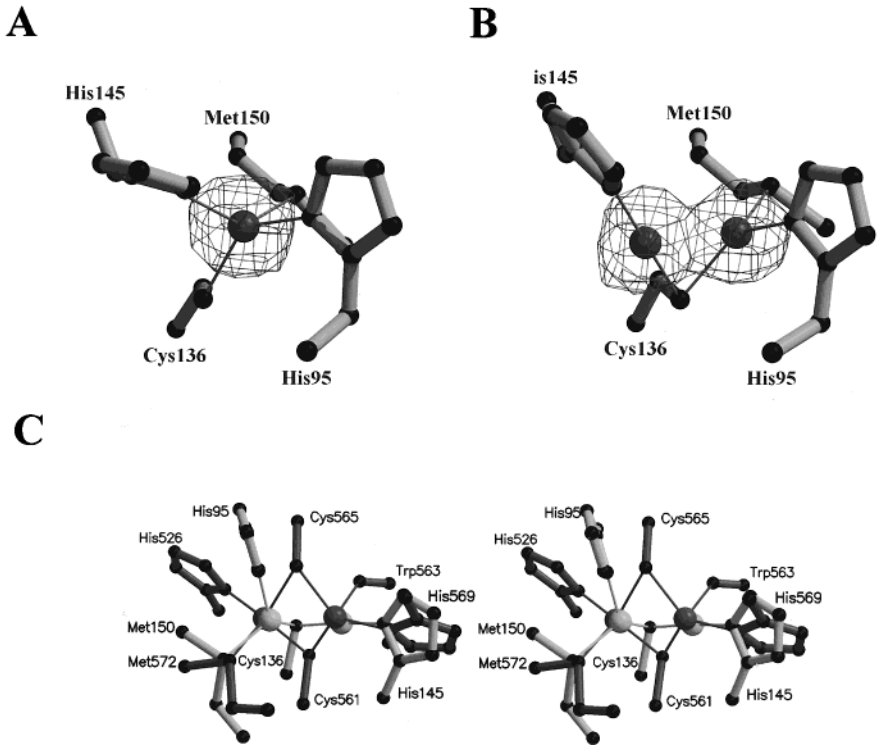

FIGURE 3: Stick diagram of the type I Cu site of (A) oxidized H255N[NO_2^-] and (B) reduced H255N[NO_2^-] AfNIR. The $F_o - F_c$ omit electron density maps surrounding the type I coppers are contoured at 5σ. (C) Stereo diagram of the modified type I Cu site of reduced H255N[NO_2^-] AfNIR superimposed on the Cu_A site of nitrous oxide reductase from *P. nautica* (*30*).

Type I Copper Site. In the oxidized D98N[NO_2^-] and H255N[NO_2^-] crystal structures, the mononuclear type I copper sites are coordinated in a distorted trigonal bipyramidal geometry by four protein ligands (His145, His95, Cys136, and Met150) (Figure 3A) as observed in native AfNIR structures (*10*, *11*, *22*). However, the type I copper site in the reduced D98N[NO_2^-] and H255N[NO_2^-] crystal structures reveals an unexpected copper coordination. In the presence of 20 mM ascorbate, 2 mM copper chloride, and 1 mM zinc acetate, the type I ligands rearrange to incorporate a second metal atom forming a dinuclear site (Figure 3B). The second metal was modeled as a copper in the structure. Crystallographic *B*-factors of 21.8 $\pm$ 0.1 Å^2 are observed for both copper atoms in the modified type I copper site in the reduced H255N[NO_2^-] structure (Figure 3B). The *B*-factors for the analogous copper atoms in the reduced D98N[NO_2^-] structure are increased approximately 30% (32.7 and 35.8 Å^2), suggesting reduced metal occupancy. In the reduced H255N[NO_2^-] structure, the side chain of His145 is shifted approximately 0.6 Å in the opposite direction of the original type I copper and is rotated approximately 35° about the χ_2 angle such that the Nδ1 atom serves as a ligand to a second copper atom (Cu500) (Figure 3B). Cys136 Sγ becomes a shared ligand between the two coppers (Cu500 and Cu501) while the Met150 Sδ and His95 Nδ1 ligands remain unperturbed. A loop incorporating residues Ala137 through His145 that packs against the type I site is displaced slightly with a root-mean-squared deviation of 0.4 Å for Cα atoms relative to the oxidized H255N[NO_2^-] structure to accommodate the second copper atom (Cu500). Pro138, the proximal residue from this loop, adopts a different pucker conformation such that the Cγ atom is 3.11 Å from Cu500. Apart from the shift in this surface loop, the tertiary structure in the modified type I copper site remains largely unchanged. Ligand−copper distances and geometries are presented in Table 3.

DISCUSSION

In this study, nitrite soaked crystal structures of two active site mutants of AfNIR (D98N and H255N) have been determined in both the oxidized and reduced forms to a resolution sufficient to observe the precise binding mode of the substrate to the copper. The observed alterations in binding mode in the oxidized structures provide significant insight into the roles of Asp98 and His255 in determining the mode of nitrite binding in the native enzyme. The reduced mutant structures are discussed primarily with respect to the surprising observation of the presence of dinuclear type I copper sites.

Role of Asp98 in Determining the Mode of Nitrite Binding. Of the residues in close proximity to the type II copper in the structure of native AfNIR in the resting state, Asp98 is the least ordered (*14*). The binding of nitrite results in a decrease in the *B*-factors of Asp98 resulting from the formation of a direct hydrogen bond to the substrate. The bidentate coordination of nitrite through the oxygen atoms to the type II copper in the oxidized D98N[NO_2^-] crystal structure is similar to that observed in the native nitrite soaked AfNIR crystal structure (*14*); however, higher *B*-factors and omit difference electron density maps indicate that both nitrite and the side chain of Asn98 are disordered [Figure 2, D98N(ox), -(red)]. In the structure of D98N AfNIR in the oxidized resting state, Asn98 is also poorly ordered (*20*). The binding of substrate to D98N AfNIR has little effect in stabilizing the conformation of this residue. Clearly, from a comparison of these structures, Asn98 is not able to form a hydrogen bond to water or substrate bound at the active site.

Table 3: Type I Copper−Ligand Bond Lengths and Geometries

parameter	oxidized D98N[NO_2^-]	reduced D98N[NO_2^-]	oxidized H255N[NO_2^-]	reduced H255N[NO_2^-]
		I. Type I Cu−Ligand Distances (Å)		
Cu500−145N$^{\delta 1}$	N/A	2.01 (0.24)[b]	N/A	1.83 (0.13)[a]
Cu500−136S$^{\gamma}$	N/A	2.08 (0.02)	N/A	2.12 (0.07)
Cu500−Cu501	N/A	2.31 (0.02)	N/A	2.45 (0.05)
Cu501−136S$^{\gamma}$	2.23 (0.03)[a]	2.25 (0.1)	2.26 (0.04)[a]	2.55 (0.45)
Cu501−95N$^{\delta 1}$	2.07 (0.02)	2.09 (0.06)	2.12 (0.06)	2.21 (0.2)
Cu501−150S$^{\delta}$	2.44 (0.01)	2.38 (0.16)	2.41 (0.05)	2.42 (0.24)
Cu501−145N$^{\delta 1}$	2.07 (0.06)	N/A	2.00 (0.08)	N/A
		II. Type I Cu−Ligand Angles (deg)		
145N$^{\delta 1}$−Cu501−150S$^{\delta}$	130 (3.0)	124 (1.0)	131 (2.0)	126 (2.0)
136S$^{\gamma}$−Cu501−95N$^{\delta 1}$	132 (1.0)	138 (5.0)	131 (1.0)	136 (6.0)
95N$^{\delta 1}$-Cu501−150S$^{\delta}$	87.7 (0.3)	96.0 (5.0)	89.8 (2.0)	98.2 (1.8)
136S$^{\gamma}$−Cu501−150S$^{\delta}$	106 (1.0)	116 (5.0)	105 (2.0)	121 (3.0)
136S$^{\gamma}$−Cu501−145N$^{\delta 1}$	105 (2.0)	84.2 (0.4)	105 (2.0)	77.5 (2.5)
145N$^{\delta 1}$−Cu501−95N$^{\delta 1}$	97.6 (1.5)	96.7 (8.8)	96.7 (1.3)	94.6 (2.1)
145N$^{\delta 1}$−Cu500−150S$^{\delta}$	N/A	103 (5.5)	N/A	113 (2.0)
145N$^{\delta 1}$−Cu500−136S$^{\gamma}$	N/A	164 (12)	N/A	171 (5.0)
145N$^{\delta 1}$−Cu500−95N$^{\delta 1}$	N/A	88.0 (4.7)	N/A	98 (4.7)
136S$^{\gamma}$−Cu500−Cu501	N/A	58.8 (4.4)	N/A	54.7 (1.6)
136S$^{\gamma}$−Cu501−Cu500	N/A	53.0 (0.7)	N/A	53.0 (2.5)
95N$^{\delta 1}$-Cu500−150S$^{\delta}$	N/A	46.9 (3.1)	N/A	46.0 (0.9)

[a] Bond distances and angles are an average of all three monomers. [b] Bond distances and angles for the reduced D98N[NO_2^-] structure are from monomers A and B.

The conformational disorder of Asn98 has been suggested by recent FT-IR CO studies of the reduced D98N AfNIR variant (*28*). From these experiments, two CO stretching frequencies were measured and identified as representing different modes of CO binding. The oxidized D98N crystal structures in the presence and absence of substrate suggest that these two CO stretching frequencies likely result from two conformations of Asn98, one of which interacts with bound CO. Similar FT-IR CO experiments of native AfNIR recorded over a pH range of 6.0−8.0 suggest that Asp98 is deprotonated, thereby requiring nitrite to bind in the protonated form to the native enzyme (*28*). These observations are consistent with five crystal structures of AcNIR solved at pH values between 5 and 6.8 that show minimal structural change in the active site (*13*). Recent steady-state kinetics show an increase in the K_m for nitrite to the D98N and D98E AcNIR mutants of 200-fold and 15-fold, respectively, indicating that a negatively charged Asp98 may be required for high-affinity binding of the substrate (*21*).

Taken together, the available data indicate that the disorder observed for nitrite and Asn98 in the oxidized D98N[NO_2^-] crystal structure is a result of the inability of the Nδ2 atom of Asn98 to form a hydrogen bond with nitrite bound in the protonated form. Furthermore, the data presented here identify the hydrogen bond between Asp98 and nitrite in the native structure as essential in anchoring nitrite in the active site for productive catalysis. This hydrogen bond is also likely to serve as a direct link through which protons are exchanged during catalysis.

Role of His255 in Determining the Mode of Nitrite Binding. The lack of a direct interaction with bound substrate suggests that His255 plays a limited role in nitrite binding; however, mutagenesis studies have shown that this residue is critical for nitrite binding and function (*19*, *21*). His255 is thought to complement electrostatically the negative charge on nitrite, donate protons to the substrate directly during catalysis, or be indirectly involved in nitrite binding through correct positioning of Asp98 through the bridging water (*13*, *14*, *16*, *19*−*21*).

In the crystal structure of H255N AfNIR in the resting state, steric constraints indicate that an additional active site water (Wat1099) bound near the copper must be displaced for correct binding of nitrite in the active site (*20*). Surprisingly, in the oxidized H255N[NO_2^-] structure, neither the ligand water (Wat503) nor the additional active site water, Wat1099, is displaced upon nitrite binding [Figure 2, H255N(ox)]. Instead, nitrite adopts a novel binding mode in the active site, displacing the weakly bound Wat2098 and coordinating to the type II copper via a single oxygen atom (Figure 2). The resulting pentacoordinate copper displays a distorted square pyramidal geometry that is similar to a synthetic analogue where two nitrogen atoms and two oxygen atoms, analogous to the ligand water and the O1 atom of nitrite, are in-plane with the copper and a third nitrogen, analogous to His306, which is positioned as the apical ligand (*29*). As shown by the low enzyme activity of the H255N mutant, the observed alternate binding mode for nitrite observed in the oxidized H255N[NO_2^-] structure is likely catalytically unproductive. However, this change in the nitrite binding mode clearly identifies His255 as an essential residue in determining the productive nitrite binding observed in the native AfNIR crystal structure.

Three major factors may determine the alternate binding mode of nitrite. First, the displacement of Wat2098, which shows high *B*-factors and is only hydrogen-bonded singly to the rest of the structure, is more energetically favorable than displacing both the additional active site water (Wat1099) and the ligand water (Wat503) that are part of an extensive solvent network (Figure 1C). Second, a hydrogen bond between nitrite and Asp98, responsible for the low average *B*-factor for nitrite and the well-defined electron density, limits the number of favorable positions of nitrite in the active site. Third, analysis of the native nitrite soaked AfNIR crystal structure (*14*) suggests that the positively charged His255

may serve to lower the pK_a and orient Asp98 through the bridging water (Wat1098) for optimal interaction with the bound nitrite. The H255N mutant would likely increase the pK_a of Asp98 such that this residue is now protonated and uncharged when nitrite is bound. Such a change in the protonation state of Asp98 may result in the altered binding mode of nitrite.

The ability of a mutation at position 255 to affect nitrite binding was observed recently from histidine and water proton ENDOR and EPR spectroscopy of H287E RsNIR (*16*, *19*). In these experiments, displacement of the ligand water by nitrite alters the spectral properties of the native enzyme. In the H287E mutant, no spectral change is observed following the addition of nitrite, suggesting a limited ability for nitrite to bind. One explanation suggested by Olesen et al. is that a charge repulsion effect exists between the negatively charged carboxylate of Glu287 and nitrite (*19*). FT-IR CO data (*28*) and steady-state kinetics (*21*) suggest a more indirect role for His255. These experiments indicate that a deprotonated, negatively charged Asp98 residue is required for high-affinity nitrite binding by serving as a proton acceptor in forming a hydrogen bond with the protonated, uncharged form of the molecule. The absence of a formal charge on nitrite likely results in limited electrostatic interactions of bound nitrite with charged active site residues such as His255. Modest increases in measured K_m values for nitrite, combined with a logarithmic decrease in the enzyme activity of His255 AcNIR mutants, are interpreted as His255 being involved indirectly in coordinating nitrite but essential in orienting Asp98 through the bridging water (*21*).

Catalytic Mechanism of Copper-Containing Nitrite Reductase. The distinctive manner in which nitrite is bound in the oxidized H255N nitrite soaked structure provides unique insight into the catalytic mechanism of copper-containing nitrite reductases. In the current mechanistic model for CuNIRs, a protonated nitrite molecule displaces the ligand water and coordinates to the type II copper prior to electron transfer from the type I copper (*20*). From Figure 4, reduction of the type II copper is followed by the formation of a transient complex in which the N−O bond of nitrite proximal to Asp98 is broken, leaving a hydroxyl group and nitric oxide (NO) simultaneously bound to a pentacoordinated copper (steps 2 and 3). In the transient pentacoordinate complex, as drawn in Figure 4, the O1 and N atoms of NO adopt similar positions to the O1 and N atoms of nitrite observed in the oxidized H255N[NO_2^-] crystal structure (inset box). In this transient complex, both Asp98 and His255 are uncharged. The subsequent protonation of the active site, possibly initiated through His255, results in the release of NO and regeneration of the water ligand to the type II copper.

The oxidized H255N[NO_2^-] structure provides evidence that the proposed transient intermediate state of the enzyme is energetically accessible. The positioning of NO and the hydroxyl bound to the type II copper modeled from the oxidized H255N[NO_2^-] structure (Figure 4, inset box) are directed favorably with respect to the active site cavity that shows a distinct polar and hydrophobic face. The positioning of nitrite in the oxidized H255N[NO_2^-] structures suggests that in the native enzyme NO is oriented for diffusion out of the active site along the side devoid of charged and polar residues and lined with hydrophobic residues beginning at

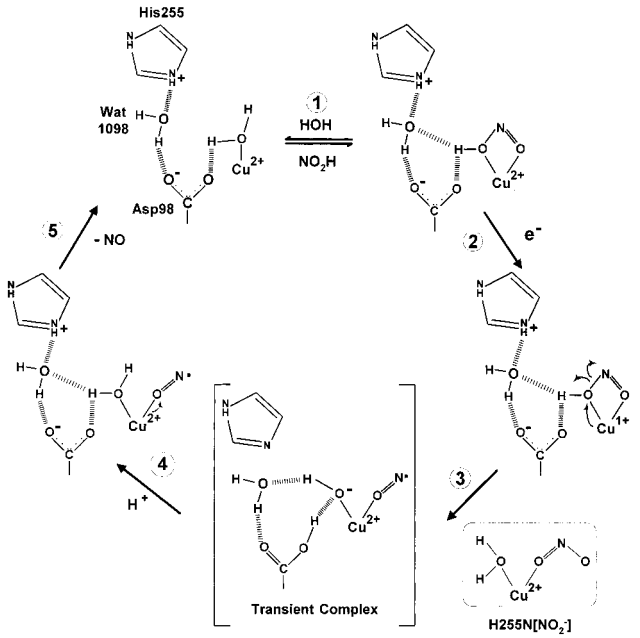

FIGURE 4: Proposed catalytic mechanism for copper-containing nitrite reductases.

Ala137, Leu308, and Val146 and extending through to Val142 and Phe312, which are located on the surface of NIR. This model of diffusion limits the interaction of NO with polar residues, thereby minimizing nonspecific side reactions. The hydroxyl group positioned proximal to the bridging water (Wat1098) is directed toward the polar side of the active site cavity that assists to stabilize the transient negative charge.

Despite the lack of noticeable reoxidation following nitrite soaking and reduction at 0 °C, the type II copper site may be partially oxidized, contributing to the observed disorder in the active site. Interestingly, the substantial increase in the *B*-factor of the bridging water (Wat1098) upon reduction of the nitrite soaked native (*14*) and D98N AfNIR structures is consistent with a previously proposed disruption of the solvent network linking residues Asp98 and His255 (*21*). This proposed disruption would permit the side chain of His255 the freedom to approach reaction intermediates and directly donate a proton during catalysis (*21*). However, modeling studies (*20*) have shown that His255 cannot be oriented to form a hydrogen bond with nitrite nor does His255 show increased *B*-factors indicative of increased mobility in reduced AfNIR crystal structures. An alternative explanation is that the proton is shuttled through the bridging water (Wat1098). In the oxidized H255N[NO_2^-] structure, the ligand water to the type II copper is positioned within hydrogen bonding distance to the bridging water (Wat1098) [Figure 2, H255N(ox)], creating a defined pathway through which protons can exchange during catalysis. A proton shuttled through the bridging water (Wat1098) during catalysis likely originates from the bulk solvent where structural data show a well-defined solvent network extending from Wat1098 to His260 that sits on the surface of NIR (*22*).

Type I Copper Site. Several different copper sites exist in proteins ranging from the mononuclear type I and II centers to the recently discovered tetranuclear Cu_Z cluster (*30*). A cupredoxin-like fold in cytochrome *c* oxidase (*31*) and nitrous

oxide reductase (*30*) coordinate a mixed-valent dinuclear copper cluster termed the Cu_A site represented by the consensus sequence {C $(X)_3$ C $(X)_3$ H $(X)_2$ M} (*32*). The reduced D98N[NO_2^-] and H255N[NO_2^-] crystal structures show that a second metal atom has been incorporated into the type I copper site, generating a unique dinuclear metal center (Figure 3A,B). This site is structurally similar to the dinuclear Cu_A site (Figure 3C), but shows unusual copper coordination. The proximity of the two metal atoms (Table 3) is consistent with spectroscopic measurements of a traditional Cu_A site that identify a 2.5 Å metal−metal bond (*31*). The coordination of the copper atoms in a traditional Cu_A site is that of a distorted tetrahedral geometry. In this site, there are two shared Cys Sγ ligands, with His Nδ1 and Met Sδ atoms completing the coordination for one copper, and His Nδ1 and a carbonyl oxygen from either a Trp (*30*) or a Glu (*33*) coordinating the second copper atom. The pseudo-dinuclear site presented here lacks the overall symmetry of a traditional Cu_A site as it incorporates only four ligands instead of six in the coordination of the two coppers.

EXAFS spectroscopy (*31*) has provided a model to compare the topological similarities and the evolutionary link between the mononuclear type I and dinuclear Cu_A sites. This connection has been demonstrated further through protein engineering studies of the blue copper protein quinol oxidase (*34*). In this study, extensive site-directed mutagenesis of the type I site loop resulted in the successful formation of a dinuclear Cu_A center from a type I copper site. To our knowledge, the dinuclear pseudo-Cu_A sites in AfNIR are the first examples of a nonengineered expansion of a type I site to a dinuclear copper site similar to a Cu_A. The small changes in structure and the flexibility of the surface loop incorporating the His145 ligand suggest that this novel dinuclear site may be physiologically attainable in NIR. Last, the introduction of such a site would alter the redox chemistry of NIR, especially if the coppers existed in a mixed-valence state as observed in the Cu_A site. Such a site could potentially be used by NIR as a mechanism to regulate activity.

Conclusions. The ability of active site residues to mediate the correct mode of nitrite binding is shown clearly in the crystal structures presented here. Despite the lack of an interaction between His255 and nitrite, the mutation of His255 to an Asn results in a restructured solvent network and a completely novel mode of nitrite binding. We suggest that this alternate binding mode mimics the electronic and structural properties of a proposed catalytic intermediate in native AfNIR. The surprising appearance of a nonengineered dinuclear type I metal site in the reduced mutant structures may be a general model for the evolution of the Cu_A site. This unusual metal coordination may also represent a physiologically relevant change during catalysis potentially used in regulating the redox chemistry and overall activity of copper-containing nitrite reductases. Further work is currently in progress to determine whether the formation of the dinuclear site is attainable in the native enzyme under physiological concentrations of copper.

ACKNOWLEDGMENT

We thank Dr. C. Cambillau for supplying the coordinates of the nitrous oxide reductase crystal structure prior to their release to the Protein Data Bank.

REFERENCES

1. Nishiyama, M., Suzuki, J., Kukimoto, M., Ohnuki, T., Horinouchi, S., and Beppu, T. (1993) *J. Gen. Microbiol. 139*, 725−733.
2. Averill, B. A. (1996) *Chem. Rev. 96*, 2951−2964.
3. Cutruzzola, F. (1999) *Biochim. Biophys. Acta 1411*, 231−249.
4. Fenderson, F. F., Kumar, S., Liu, M.-Y., Payne, W. J., and LeGall, J. (1991) *Biochemistry 30*, 7180−7185.
5. Kakutani, T., Watanabe, H., Arima, K., and Beppu, T. (1981) *J. Biochem. 89*, 453−461.
6. Abraham, Z. H., Lowe, D. J., and Smith, B. E. (1993) *Biochem. J. 295*, 587−593.
7. Michalski, W. P., and Nicholas, D. J. D. (1985) *Biochim. Biophys. Acta 828*, 130−137.
8. Hoffmann, T., Frankenberg, N., Marino, M., and Jahn, D. (1998) *J. Bacteriol. 180*, 186−189.
9. Kobayashi, M., and Shoun, H. (1995) *J. Biol. Chem 270*, 4146−4151.
10. Godden, J. W., Turley, S., Teller, D. C., Adman, E. T., Liu, M. Y., Payne, W. J., and LeGall, J. (1991) *Science 253*, 438−442.
11. Kukimoto, M., Nishiyama, M., Murphy, M. E. P., Turley, S., Adman, E. T., Horinouchi, S., and Beppu, T. (1994) *Biochemistry 33*, 5246−5252.
12. Suzuki, S., Kohzuma, T., Deligeer, Yamaguchi, K., Nakamura, N., Shidara, S., Kobayashi, K., and Tagawa, S. (1994) *J. Am. Chem. Soc. 116*, 11145-11146.
13. Adman, E. T., Godden, J. W., and Turley, S. (1995) *J. Biol. Chem. 270*, 27458−27474.
14. Murphy, M. E., Turley, S., and Adman, E. T. (1997) *J. Biol. Chem. 272*, 28455−28460.
15. Howes, B. D., Abraham, Z. H. L., Lowe, D. J., Brüser, T., Eady, R. R., and Smith, B. E. (1994) *Biochemistry 33*, 3171−3177.
16. Veselov, A., Olesen, K., Sienkiewicz, A., Shapleigh, J. P., and Scholes, C. P. (1998) *Biochemistry 37*, 6095−6105.
17. Strange, R. W., Murphy, L. M., Dodd, F. E., Abraham, Z. H., Eady, R. R., Smith, B. E., and Hasnain, S. S. (1999) *J. Mol. Biol 287*, 1001−1009.
18. Strange, R. W., Dodd, F. E., Abraham, Z. H. L., Grossman, J. G., Brüser, T., Eady, R. R., Smith, B. E., and Hasnain, S. S. (1995) *Nat. Struct. Biol. 2*, 287−292.
19. Olesen, K., Veselov, A., Zhao, Y., Wang, Y., Danner, B., Scholes, C. P., and Shapleigh, J. P. (1998) *Biochemistry 37*, 6086−6094.
20. Boulanger, M. J., Kukimoto, M., Nishiyama, M., Horinouchi, S., and Murphy, M. E. P. (2000) *J. Biol. Chem 275*, 23957−23964.
21. Kataoka, K., Furusawa, H., Takagi, K., Yamaguchi, K., and Suzuki, S. (2000) *J. Biochem. 127*, 345−350.
22. Murphy, M. E. P., Turley, S., Kukimoto, M., Nishiyama, M., Horinouchi, S., Sasaki, H., Tanokura, M., and Adman, E. T. (1995) *Biochemistry 34*, 12107−12117.
23. Otwinowski, Z., and Minor, W. (1997) *Methods Enzymol. 276*, 307−326.
24. Brunger, A. T. (1997) *Methods Enzymol. 277*, 366−404.
25. Brunger, A. T., Adams, P. D., Clore, G. M., Delano, W. L., Gros, P., Grosse-Kunstlere, R. W., Jiang, J. S., Kuszewski, J., Nilges, N., Pannu, S., Read, R. J., Rice, L. M., Simonson, T., and Warren, G. L. (1998) *Acta Crystallogr. D54*, 905−921.
26. Laskowski, R. A., MacArthur, M. W., Moss, D. S., and Thornton, J. M. (1993) *J. Appl. Crystallogr. 26*, 283−291.
27. Jones, T. A., Zou, J.-Y., Cowan, S. W., and Kjeldgaard, M. (1991) *Acta Crystallogr. A47*, 110−119.
28. Zhang, H., Boulanger, M. J., Mauk, A. G., and Murphy, M. E. P. (2000) *J. Phys. Chem. B 104*, 10738−10742.
29. Halfen, J. A., and Tolman, W. B. (1994) *J. Am. Chem. Soc. 116*, 5475−5476.
30. Brown, K., Tegoni, M., Prudencio, M., Pereira, A. S., Besson, S., Moura, J. J., Moura, I., and Cambillau, C. (2000) *Nat. Struct. Biol. 7*, 191−195.

31. Blackburn, N. J., Barr, M. E., Woodruff, W. H., van der Ooost, J., and de Vries, S. (1994) *Biochemistry 33*, 10401−10407.
32. Zumft, W. G., Dreusch, A., Lochelt, S., Cuypers, H., Friedrich, B., and Schneider, B. (1992) *Eur. J. Biochem 208*, 31−40.
33. Tsukihara, T., Aoyama, H., Yamashita, Y., Tomizaki, R., Yamagauchi, H., Shinzawa-Itoh, K., Nakashima, R., Yaono, R., and Yoshikawa, S. (1995) *Science 269*, 1069−1074.
34. Wilmanns, M., Lappalainen, P., Kelly, M., Sauer-Eriksson, E., and Saraste, M. (1995) *Proc. Natl. Acad. Sci. U.S.A. 92*, 11955−11959.
35. Kraulis, P. (1991) *J. Appl. Crystallogr. 24*, 946−950.
36. Merritt, E. A., and Murphy, M. E. P. (1994) *Acta Crystallogr. D50*, 869−873.

BI0107400